Assembly of Gold Nanoparticles into Microwire Networks Induced by Drying Liquid Bridges

Ivan U. Vakarelski,[1,2,*] Derek Y. C. Chan,[3,4] Takashi Nonoguchi,[1] Hiroyuki Shinto,[1] and Ko Higashitani[1,†]

[1]*Department of Chemical Engineering, Kyoto University, Katsura, Nishikyo-ku, Kyoto 615-8510, Japan*
[2]*Institute of Chemical and Engineering Sciences, 1 Pesek Road, Jurong Island, 627833, Singapore*
[3]*Particulate Fluids Processing Centre, University of Melbourne, Parkville, Victoria 3010, Australia*
[4]*Department of Mathematics, National University of Singapore, 117543, Singapore*

(Received 23 October 2008; published 4 February 2009)

Large interconnected gold wire structures ($\sim$cm^2) of different topologies have been made by the drying of a gold nanoparticle suspension that has formed a connected network of liquid bridges in the interstices between a 2D crystalline layer of latex particles and a substrate. Slow evaporation of the suspending medium assembles the nanoparticles into a periodic or disordered conducting network of micrometer thick gold wires on the substrate. The presence of surfactants in the suspension is critical to maintaining the stability of the liquid bridge network during the evaporation process.

DOI: 10.1103/PhysRevLett.102.058303 PACS numbers: 47.57.J−, 47.55.nk, 68.03.Fg, 81.16.Dn

The development of robust and inexpensive micropatterning methods based on particle array templates is of continuing interest in both fundamental research and technological applications [1,2]. State of the art methods such as photolithography, soft lithography, and nanoimprint have achieved impressive results in producing patterns and features down to the nanometer range [3,4]. However, these methods generally involve multiple step processes that require complex and costly production facilities. Here we report a simple ''bench top'' drying lithography method based on the evaporation of a suspension of gold nanoparticles ($\sim$20 nm diameter) that has formed a connected liquid bridge network in the interstices between a 2D crystalline layer of polystyrene latex particles (50–100 μm diameter) and a substrate. Slow evaporation of the suspending liquid assembles the gold nanoparticles into a connected micorwires network on the substrate that can span areas of square centimeters. Depending on the pretreatment of the 2D crystalline polystyrene latex mask, the morphology of the resulting network on a flat substrate can be disordered [Figs. 1(a) and 1(b)] or highly ordered [Fig. 1(c)]. Such networks can also form on 3D substrates such as on top of another crystalline latex substrate [Fig. 1(d)]. We will also demonstrate that added surfactant is critical to the formation of networks with good connectivity.

A primary motivation is the production of transparent conducting coatings that can serve as an alternative to industry standard vacuum deposited indium tin oxide. The high cost and limited supply of indium has stimulated the quest for other novel solutions, including the use of coatings based on carbon nanotubes, conductive polymers, and metal nanoparticles [5–7]. Microwire networks based on metal nanoparticles or other materials is expected to significantly improve the conductance-transparency characteristic of the layer.

Evaporation of drying droplets has been used to assemble nanoparticles, nanotubes, diblock copolymers, or DNA liquid crystals [8–12]. Harris *et al.* [13,14] pioneered the use of prefabricated micropattern masks placed over a particle suspension film to induce a spatially varying evaporation rate that resulted in desired spatial patterns of assembled particles after evaporation. In the present approach, the 2D latex particle crystal deposited on a substrate also has a similar role as an evaporation mask. But more importantly, the spatial disposition of the latex particles on the substrate, which can be altered for instance by first heating the substrate to increase the area of contact between the latex particles and the substrate, serves as a template for different liquid bridge's network topologies formed by an aqueous suspension of gold nanoparticles.

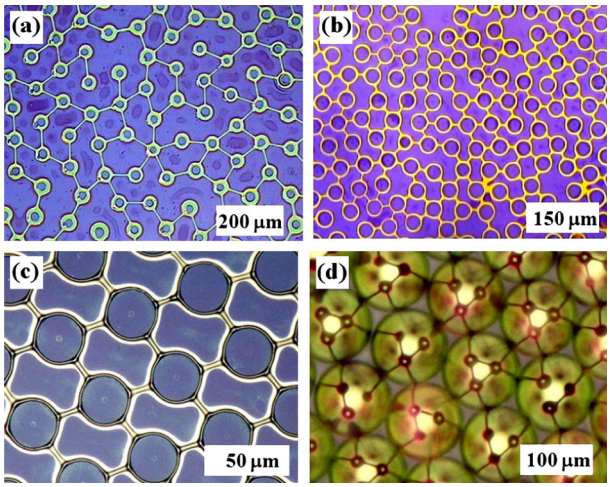

FIG. 1 (color online). Microscopic images of disordered and ordered microwire patterns formed on substrates by evaporative assembly of a gold nanoparticle suspension using (a) 100 μm, (b) and (c) 50 μm latex particles template on planar glass surfaces, and (d) microwire patterns on a monolayer of 100 μm latex particles. Images (a), (b) were taken from the bottom of the substrate and (c), (d) were top observations.

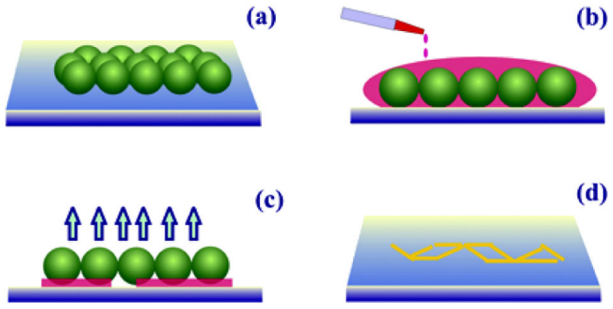

FIG. 2 (color online). Schematic of the lithography procedure: (a) 2D latex particle crystal template on a glass slide, (b) doping with gold nanoparticle suspension, (c) drying, and (d) latex particles removal.

The major steps of our lithographic procedure are illustrated in Fig. 2. The latex particle templates were first produced by the drying of a droplet of the aqueous monodisperse latex suspension (50 μm or 100 μm diameter polystyrene microspheres purchased from Duke Scientific Corp.) that has been spread over the surface of a thoroughly cleaned microscope glass slide. The latex particle concentration was adjusted to ensure near monolayer surface coverage. Because of capillary forces, 2D crystals of a few square centimeters in size were formed after evaporation with domains (typically mm size) of 2D close-packed particles [2,15,16]. Next using a micropipette, the dried template was then doped with a fixed amount of an aqueous suspension of gold nanoparticles (Au NP) (~20 nm diameter, copolymer stabilized by Nippon Paint) and allowed to dry. The experimental parameters were Au NP concentration of 2 wt% to 6 wt% for a 3 μl/cm^2 doping suspension, a glass substrate water contact angle smaller than 45° and drying temperature of 4 °C to 25 °C at ambient humidity of 60% to 80%. When drying is complete, the template latex particles were removed using sticky tape to expose the underlying Au microwire patterns that have been deposited on the substrate (Fig. 1).

The dynamics of the evaporation of the Au NP suspension was monitored by top view microscopy observations and by inverted microscopy imaging through the glass substrate. Top view observations reveal that initially, the Au NP suspension film covers the 2D latex crystal entirely. The set of contact points between the latex particles and the substrate are seen as a regular hexagonal array of small bright circular dots in inverted microscopy images [Fig. 3(a)]. As the liquid evaporates, the top of the latex particles starts to protrude through the film meniscus surface. This receding surface meniscus is then stretched between the latex particles until the meniscus interface between the latex particles falls below the equatorial plane of the latex particles and becomes thin enough to form ''holes'' that expose the air-substrate interface surrounded by the air-liquid-substrate three-phase contact line. The air-substrate areas or holes observed in the inverted microscopy images are seen as lighter parts of the micrographs (Figs. 3(a)–3(c)). The remaining liquid bridge network seen as the dark portions of the micrographs is made up of long liquid drops or bridges on the substrate that join the pendular rings of liquid around the base of latex particles where they are in contact with the substrate [16].

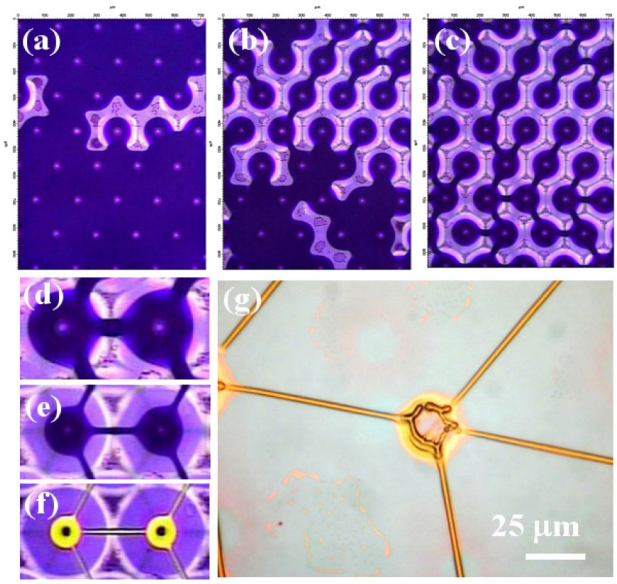

FIG. 3 (color online). (a),(b),(c) Consecutive microscopy snapshots viewed from the bottom of the substrate on a 400 × 650 μm area of the latex particle crystal that tracks the formation of the liquid bridge network on the substrate. The light dots mark the latex particle-glass contacts and the bright opening the progression of the air-substrate area. (d),(e),(f) 100 × 200 μm images of the evaporative thinning stages of a single liquid bridge on the substrate that joins two pendular rings of liquid at the base of two neighboring latex particles and the final assembly of Au NP into a microwire joining the ''nodes'' around the base of the latex particles. (g) Top view microscopy image of a microwire node that resembles a solder spot after removal of the template latex particles. The microwires are all connected at the base of the node on the substrate as seen in (d)–(f). (See supplementary material for a video of the entire process [18].)

The exposed areas of substrate-air interface, seen as bright portions of the micrographs [Figs. 3(a)–3(c)], first appear at the places of the largest interparticle separations or at missing or dislocated crystal particle sites. Thereafter the air-substrate openings grow and propagate along the surface by breaking into the neighboring interparticle cell space in a process that is similar to invasion percolation [17]. New air-substrate openings also develop at other locations throughout the 2D latex crystal. A movie that shows the progression from Figs. 3(a)–3(f) is provided as supplementary material [18]. When such openings cannot propagate any further, a stable liquid bridge network that connects all latex particles will result [Fig. 3(c)] and then thins down slowly without further breakage until the

final consolidation into microwire structures shown in Figs. 3(d)–3(f).

Examples of microwire patterns on a planar substrate using 100 μm and 50 μm latex particles are given in Figs. 1(a)–1(c). The dimension of the circular shape in the nodes was controlled by changing the particle-substrate contact area via heating, e.g., by annealing the glass slides for several minutes on a heated plate during the final stage of the latex particle template preparation. By using two layers of latex particle crystals, it is also possible to cover the 3D surface of the lower layer of latex particles by a microwire network as seen in Fig. 1(d) where the upper latex layer has been removed. This demonstrates that such microwire can be formed on both flat as well as 3D substrates and possibly even throughout a 3D particle crystal.

The degree of connectivity of the microwire network is determined by two independent processes. The first is the initial evaporation of the nanoparticle suspension to the stage of exposing holes of air-substrate areas that are separated by the liquid bridge network that connects the 2D template of the latex particle. The second process is the final thinning of the liquid bridge network that concentrates and assembles the Au NP into continuous wire structures that connects the ring of Au NP formed at the base of each latex template particle.

During the first process of the formation of holes of air-substrate areas between the latex particles shown in Figs. 1(a)–1(c), the air-water interface of the liquid network has local radii of curvature of opposite signs at the liquid bridge on the substrate between particles and at the pendular ring at the base of the latex particle-substrate contact. The proximity of surfaces with opposing radii of curvature will help minimize the pressure difference between the liquid and the vapor phase and hence facilitate slow evaporation. The creation of an air-substrate hole between three latex particles in an equilateral triangular configuration requires higher local curvatures of the air-liquid interface than if a liquid bridge is broken to allow the air-substrate hole to form in the interstitial space formed by four latex particles. This is in accord with the observed stability of rhombic unit cell seen in Fig. 1(c) and that no air-substrate holes have been observed to appear inside the equilateral triangle bounded by three liquid bridges joining the three nearest neighbor latex particles.

During the second process of the thinning of the liquid network shown in Figs. 3(d)–3(f), the long linear liquid bridges on the substrates that join the pendular rings at the base of the particles must remain intact and not break up. An equilibrium stability analysis of such linear liquid bridges on a flat substrate with the assumption of constant surface tension and contact angles shows that they are unstable and will always break up [19]. However, our further investigation of the stability of such liquid bridges formed by water or 2-propanol shows that neither surface tension nor the presence of low concentration of Au NP is important in determining the stability of the liquid bridge, but rather the presence of surfactant in the solution is a key factor. This implies that the present method can be readily applied to a broad range of systems that may require the use of aqueous and nonaqueous solvents.

The effects of surface tension and of surfactants on the evaporation stability of a single liquid bridge (without Au NP) on the substrate between two latex particles are demonstrated in Fig. 4. We see that liquid bridges formed from pure water (surface tension 72 mN/m) or from pure 2-propanol (surface tension 21 mN/m) are both unstable and break up when the width to length ratio is between 1/2 to 1/3, in general agreement with the pure liquid meniscus instability theory [18]. But if 0.1 mM of the surfactant sodium dodecyl sulfate (SDS) is first added to both liquids, the liquid bridges remain stable for both solutions during the entire evaporation process. These observations demonstrate that interfacial tension and contact angle, both of which are affected by the added surfactant, do not directly determine the ultimate stability of liquid bridges. However, as the solvent evaporates, the concentration of surfactant will increase substantially with that result that the ''liquid'' bridge will become more ''gel'' like which can then impart mechanical stability against breakage. The SDS should remain in the liquid phase as it is not expected to deposit on the glass substrate that carries the same charge as the surfactant. In the Au NP suspension the copolymer that stabilizes the nanoparticle suspension plays the role of the surfactant that stabilizes the liquid bridges. The inherent but important large variations in interfacial and rheological

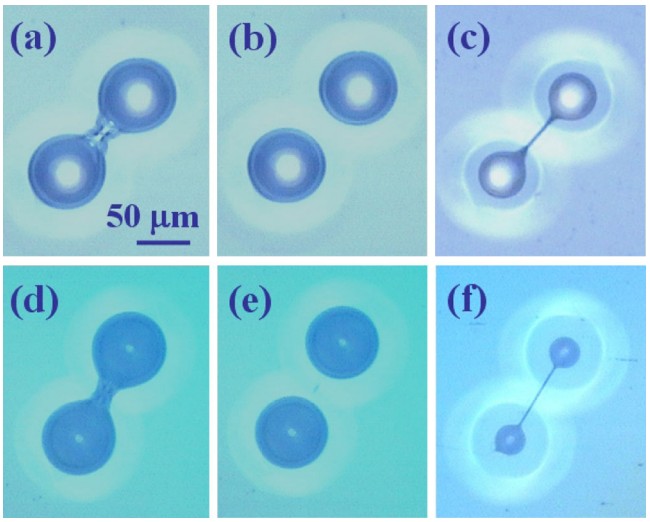

FIG. 4 (color online). Microscopy images from the bottom of the substrate of stable and unstable liquid bridges formed on the substrate (coincident with the focal plane) joining the pendular rings at the base of two contacting latex particles. Liquid bridges formed from (a), (b) pure water (surface tension 72 mN/m) and (d), (e) pure 2-propanol (surface tension 21 mN/m) break up during drying but remain stable when 0.1 mM of SDS was first added to the (c) water and (f) 2-propanol.

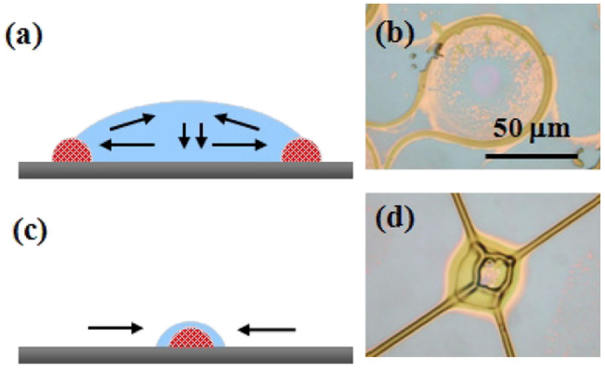

FIG. 5 (color online). Schematic diagram of (a) fast drying with meniscus pinning by nanoparticle agglomeration at the three-phase contact line and (c) slow drying that leads to solute nanoparticle consolidation. Examples for drying pattern around a 100 μm latex particle at (b) 90 °C and (d) 4 °C that illustrates the corresponding cases.

properties of the liquid during evaporation pose significant challenges in formulating a simple model to describe the process.

A low evaporation rate is also an important factor to facilitate the formation of microwire networks because of the need to prevent the ''coffee ring'' effect where insoluble particles in a suspension tend to accumulate at the retreating three-phase contact line [20,21]. This is illustrated in Fig. 5 where the slow evaporation rate at 4 °C allowed the gold nanoparticles sufficient time to diffuse into the interior of the drop while a high evaporation rate at 90 °C did result in ''coffee ring'' patterns.

A prime target application of the bridging lithography is to create transparent conductive networks. For the rhombic network shown in Fig. 1(c) the unit cell can be modeled as a resistor network of resistances R_c and R_s: where R_c is the resistance of a quarter circle segment and R_s the resistance of a straight segment. If the measurement bus bars connect one straight segment per unit cell, the resistance per cell is $(R_c + R_s)$, and if the bus bars connect two straight segments per unit cell, the resistance per cell is $2(R_c + R_s)$. Taking typical values of wire dimensions in the 50 μm to 100 μm particles networks: length of 25 μm to 50 μm, width of 2 μm to 4 μm, and height of 1 μm to 2 μm and the Au specific resistance of 22 nΩm we estimate a resistivity in the range 0.5 Ω to 1.0 Ω per unit cell of a perfect rhombic lattice, or per square area of substrate (Ω/sq). The corresponding transparency estimated as a percentage of surface area covered by the micorwires is more than 80%. This theoretical limit compares favorably with indium tin oxide coatings which have a few to several tens of Ω/sq at the same transparency range.

Preliminary measurements of our gold microwire networks showed that the samples have resistivity in the range of tens to hundreds of Ω/sq and transparency of more then 85%. These studies are ongoing and await detailed analysis with respected to the connectivity of such networks. Further details on the method performance enhancement strategies will be published elsewhere.

We expect that the liquid bridging patterning technique introduced here has the potential to lead to a number of practical developments and as well provoke further interest in the fundamental understanding of suspension drying through porous media. Behind the conductive microwire's networks other directions of developing a functional network can include the use of semiconducting or magnetic particles, nanotubes, DNA, proteins, and polymer molecules to introduce more specific network and node properties. It will also be interesting to probe the extent the process can be scaled down using smaller particles as templates.

This work is supported in part by the Sanyo Chemical Industries Ltd., the Japan Science and Technology Agency (JST), and the Australian Research Council. We acknowledge Nippon Paint for providing the gold nanoparticle's suspension.

*ivakarelski@gmail.com
†k_higa@cheme.kyoto-u.ac.jp

[1] F. Burmeister *et al.*, Adv. Mater. **10**, 495 (1998).
[2] B. G. Prevo, D. M. Kuncicky, and O. D. Velev, Colloids Surf. A **311**, 2 (2007).
[3] B. D. Gates *et al.*, Chem. Rev. **105**, 1171 (2005).
[4] Z. Nie and E. Kumacheva, Nature Mater. **7**, 277 (2008).
[5] Z. Wu *et al.*, Science **305**, 1273 (2004).
[6] D. Zhang *et al.*, Nano Lett. **6**, 1880 (2006).
[7] J. Sun, W. W. Gerberich, and L. F. Francis, Progress in Organic Coatings **59**, 115 (2007).
[8] E. Rabani, D. R. Reichman, P. L. Geissler, and L. E. Brus, Nature (London) **426**, 271 (2003).
[9] M. Kimura *et al.*, Langmuir **19**, 9910 (2003).
[10] E. R. Dufresne *et al.*, Phys. Rev. Lett. **91**, 224501 (2003).
[11] V. V. Tsukruk, H. Ko, and S. Peleshanko, Phys. Rev. Lett. **92**, 065502 (2004).
[12] I. I. Smalyukh *et al.*, Phys. Rev. Lett. **96**, 177801 (2006).
[13] D. J. Harris, H. Hu, J. C. Conrad, and J. A. Lewis, Phys. Rev. Lett. **98**, 148301 (2007).
[14] D. J. Harris and J. A. Lewis, Langmuir **24**, 3681 (2008).
[15] N. D. Denkov *et al.*, Langmuir **8**, 3183 (1992).
[16] P. A. Kralchevsky and K. Nagayama, *Particles at Fluid Interfaces and Membranes* (Elsevier, Amsterdam, 2001).
[17] D. Y. C. Chan, B. D. Hughes, L. Paterson, and C. Sirakoff, Phys. Rev. A **38**, 4106 (1988).
[18] See EPAPS Document No. E-PRLTAO-102-042907 for a movie that shows the progression from Fig. 3(a) to 3(f). For more information on EPAPS, see http://www.aip.org/pubservs/epaps.html..
[19] D. Langbein, J. Fluid Mech. **213**, 251 (1990).
[20] R. D. Deegan *et al.*, Nature (London) **389**, 827 (1997).
[21] W. D. Ristenpart *et al.*, Phys. Rev. Lett. **99**, 234502 (2007).